

# Analysis of Mixing Efficiency of Rushton Turbines Based on CFD Models

58(2), pp. 93-102, (2014)

DOI: [10.3311/PPch.2187](https://doi.org/10.3311/PPch.2187)

Creative Commons Attribution 

Bálint Molnár<sup>1\*</sup> / Attila Egedy<sup>1</sup> / Tamás Varga<sup>1</sup>

RESEARCH ARTICLE

RECEIVED 30 JUNE 2013; ACCEPTED AFTER REVISION 31 JANUARY 2014

## Abstract

*The required power and the flow pattern in a vessel mostly depend on the impeller geometry. In the literature, there are only recommendation and no indices to help choosing the proper impeller for a defined mixing task. And it is not possible to determine the optimal rotating speed for impellers applied in different mixing tasks.*

*The primary goal of our research is to compare the quantitative characterization of the level of homogeneity in a stirred system obtained by using different impeller geometries and rotating speed. Therefore, the developed flow patterns are characterized by logarithmic histogram of the distribution of velocity field. To validate the proposed characterization technique the mixing time resulted by the different geometries are also calculated. The comparison of the mixing efficiency based on the determined power number. All these models require some measurements to be validated. Hence, a laboratory experimental system was built to measure the power consumptions of the investigated impellers.*

## Keywords

*mixing efficiency · CFD · mixing time · homogeneity characterization · impeller geometry*

## Introduction

Stirred vessels are among the most commonly used pieces of equipment in chemical, food and pharmaceutical engineering fields since their good mixing ability and scale-up characteristics. Stirred vessels can be classified in different ways. They can be sorted by the way of operation of the unit (batch, semi-batch, continuous), by thermal operation (isotherm, adiabatic), or by the type of the applied impeller (turbine, jet, blade, etc.).

The most of stirred units are parts of an existing technology, so it can be difficult to obtain experimental information or collect any kind of data during the production. Hence, to build an accurate and validated model of the mixed system can require so much time which cannot be afford nowadays. The experiments in pilot plant or laboratory scale can support the modelling process. However, in these cases the scale-up of the vessel to industrial scale can be a problem, because the developed flow pattern of scale-up levels can be significantly different. Due to the developments in computer technology the operation of equipments can be studied in details without disrupting the production by using Computational Fluid Dynamics (CFD) tools. The most important advantage of the CFD approach is the possibility to model entire geometries in three dimensions, even multiphase systems [1]. CFD simulators can be applied not only in development [2], safe operation [3] and modelling the hydrodynamic behaviour of the investigated system, but after the integration of the mathematical descriptions of considered phenomenon it can describe mass and energy related transport processes, too [4]. Based on the detailed hydrodynamic modelling of the system the critical parameters and operation limits can be determined. Using adequate models the practical knowledge can be expanded, and can lead to a better understanding of the behaviour of stirred vessels, and the macro mixing phenomenon.

In the beginning, the impracticability of a direct mathematical approach to describe the required power based on the properties of the impeller and the agitation an empirical correlation was determined. However, the subject has much in common with the well-substantiated methods of analysis in fluid dynamics and, with the aid of dimensional analysis and the theory

<sup>1</sup>University of Pannonia

Egyetem u. 10., H-8200 Veszprém, Hungary

\*Corresponding author, e-mail: [molnar.balint.0106@gmail.com](mailto:molnar.balint.0106@gmail.com)

of models, a framework has been developed which satisfactorily encounters most of the flow related problems. In the late nineteenth century the first work on the power characteristics of rotating impellers can be found. The general dimensionless equation for agitator power was derived by the early researchers using dimensional analysis (Equation (1)). It was considered that impeller power should be a function of the geometry of the impeller ( $D, p, n, w, r$ ) and the tank ( $T$ ), the properties of the mixed material ( $\rho, \mu$ ), the rotational speed of the impeller ( $N$ ), and gravitational force ( $g$ ) [5,6,7].

$$f\left(\frac{D^2 \cdot N \cdot \rho}{\mu}, \frac{D \cdot N^2}{g}, \frac{P \cdot g_c}{\rho \cdot N^3 \cdot D^5}, \frac{D}{T}, \frac{D}{Z}, \frac{D}{C}, \frac{D}{p}, \frac{D}{w}, \frac{D}{r}, \frac{n_2}{n_1}\right) = 0 \quad (1)$$

Equality of all groups in Equation (1) assures similarity between systems of different size. The most important types of similarity are the kinematic and the dynamic similarities of the systems. Two systems are dynamically similar when ratios of all corresponding forces are equal, and kinematic similarity requires that velocities at corresponding points be in the same ratio. In case of geometrically similar systems, Equation (1) may be stated as

$$f\left(\frac{D^2 N \cdot \rho}{\mu}, \frac{D \cdot N^2}{g}, \frac{P \cdot g_c}{\rho \cdot N^3 \cdot D^5}\right) = 0 \quad (2)$$

Equality of the groups in this expression insures dynamic and kinematic similarity. This relationship was derived by dimensional analysis, but the same dimensionless groups may also be obtained from the Navier-Stokes equation. A complete discussion of the derivation and application of the Navier-Stokes equation is given in standard references [8,9] and will not be presented here. The analytical solution of the Navier-Stokes equations to describe the complex, three-dimensional flow in a mixing system cannot be obtained. However, the equations may be stated in dimensionless form as follows:

$$F\left(\frac{L \cdot v \cdot \rho}{\mu}, \frac{v^2}{L \cdot g}, \frac{\Delta p}{\rho \cdot v^2}\right) = 0 \quad (3)$$

The first group in Equation (3), is the Reynolds number and represents the ratio of inertial forces to viscous forces. Since this ratio determines whether the flow is laminar or turbulent, Reynolds number is a critical group in correlations can be used in calculating power consumptions. In similar systems, any convenient velocity and length may be used in the Reynolds number, which results in Equation (4).

$$\text{Re} = \frac{D^2 \cdot N \cdot \rho}{\mu} \quad (4)$$

The second group of Equation (3) is known as the Froude number and represents the ratio of inertial to gravitational forces. Equation (5) is given the Froude number for an agitator:

$$\text{Fr} = \frac{N^2 \cdot D}{D \cdot g} \quad (5)$$

Most agitation operations are carried out with a free liquid surface in a tank. The shape of the surface and, therefore, the flow pattern in the vessel, are affected by the gravitational field. This is particularly noticeable in unbaffled tanks where vortices appear; the shape of the vortex represents the balance of gravitational and inertial forces.

The third component in Equation (3) is 'the pressure coefficient' and represents the ratio of pressure differences producing flow to inertial forces. In practice the pressure distribution is not known, but in dynamically similar systems it can be shown that  $\Delta p$  and power are related. Making this substitution into the pressure coefficient together with the reference velocity gives Equation (6), which is the Power number for agitators.

$$Po = \frac{P}{\rho \cdot N^3 \cdot D^5} \quad (6)$$

Electric energy consumption is a significant part of the operating cost and also an important factor in the design of reactors, stirred vessels. It is defined as the amount of electric energy require in a period of time, in order to generate the movement of the fluid within a vessel by means of mechanic or pneumatic agitation. The costs associated with power drawn contribute significantly to the overall operation costs of industrial plants. Therefore it is desired that the mixing process is performed efficiently with a minimum expense of energy [10].

For most low viscosity fluids in equipment of conventional geometry, power requirement of mixing can be calculated directly by using a basic impeller rating and correcting with the liquid density and viscosity. Although, in different cases a more exact method of deriving power data is necessary. The first techniques are used for power draw measurements performed by wattmeters and ammeters [11]. There are simple methods, where little instrumentation is required. However, in laboratory-scale tanks, the energy loss occurring in the agitation system can be significant (even the 70% of the total power supply). Therefore, it is necessary to determine efficiency and power factor of the applied impellers. To correct the losses, calorimetric measurements are applied based on energy balance. According to Oosterhuis et al. [12], the heat energy loss (through the wall) calculated by the energy balance is only 1% of the invested energy. It is a very precise technique, but it requires high sensitivity instrumentation and the positions of thermistors within the tank must be carefully chosen.

An alternative way of measuring the power draw in mixed tanks is by the use of dynamometers, which is based on Newton's third law [13]. This method can cover wide torque range, but has a high installation cost. However, power distribution for each impeller cannot be determined in multiple agitation systems [14].

The torque meter is widely used at industrial level as well as in research laboratories. Torque meters can be adapted for measurements of torque, velocity, force, pressure and fluid flow [15].

Advantages of this device are that it can be applied in wide range of torque, and it requires little instrumentation. Although, in systems with multiple agitators, the measurement of independent power draw cannot be unbounded with this technique. Only strain gauges can measure independent power measurement [16].

Mixing is a common operation in the chemical and process industries. The objective is to take two or more miscible fluids and blend them to a predetermined degree of homogeneity. The time taken to reach this degree of homogeneity is the mixing time. The degree of mixing can be evaluated in qualitative or quantitative ways, which for several methods have been developed in recent decades. Based on the aim of the mixing there can be different techniques which can be applied to measure the homogeneity of the mixed phase (laser-induced fluorescence [17]; conductivity probes [18]; temperature probes). Hence, the mixing time measurements are applied more often, but gathering information on the homogenization of the stirred phase gains more and more ground.

Mixing time is the time taken from that moment when a specific volume of fluid is added to the fluid in the mixed vessel and blended in it with a pre-chosen degree of uniformity [19]. Various methods were developed to study the mixing time. One of these methods is the flow visualization technique [19]. The simplest (cost effective) way for examining flow patterns in a mixed system is light sheet visualization. A narrow light sheet is shone through the mixing vessel, illuminating reflective tracer particles in the fluid. This can also be videotaped [20]. Further refinements of this technique include the use of laser with a rod prism. Quantitative measurement of the mixing time based on addition of chemicals with different property to the bulk. Depending on the sampling techniques off-line, Schlieren-effect based [21], thermocouple-based [22], and conductivity probe mixing time measurement [23] can differentiate.

Stirred equipments can be qualified by a mixing coefficient. One of these methods based on the fact when two reactive fluids are brought together, reaction cannot proceed until the reactive molecules are stirred intimately on a molecular level. The product distribution from the reactions will therefore reflect the mixing history; and with the use of suitable mixing models, these distributions can be used to back-calculate mixing rates [24].

In our work the 3D mathematical models of the investigated batch reactors have been implemented in a commercial CFD software package, COMSOL Multiphysics. The impeller geometry and the number of the blades are analysed based on physical and simulation experiments. Different Rushton turbine impellers were investigated and implemented into our model. The proposed measure of the vessel homogeneity is based on the logarithmic histogram of velocity field developed in the stirred system. The simulation extends to the analyses of physical properties of the stirred phase (density, viscosity) and the rotational speed of the impeller. The electric power consumption of all the investigated impellers was defined.

## Experimental and modelling methods

### Experimental mixed system

A laboratory measurement system was developed for model validation purposes. The developed system contains a 1 litre glass reactor, one computer-controlled IKA Eurostar Power-Control Visc mixing motor, and different plastic impellers made by 3D prototype printer based on CAD drawings. Figure 1(a) shows the experimental apparatus. A torque sensor was integrated to the impeller motor, so based on the measured torque data and angular velocity values the power requirement can be calculated. Torque measurements of Rushton turbines with different number of blades were investigated at different rotational speeds, and the power absorbed by the electric mixing motor was measured too with an electric consumption meter.

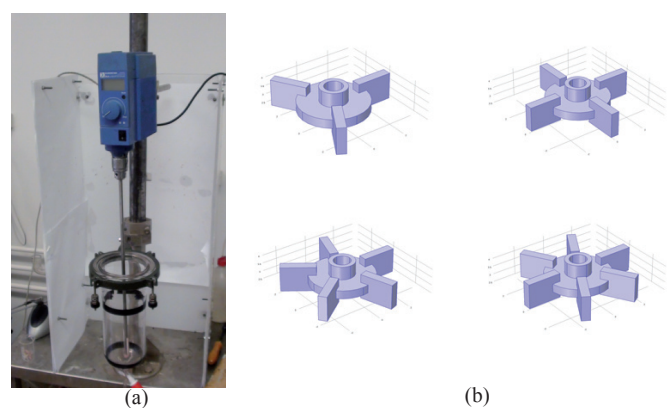


Fig. 1. (a) Experimental apparatus (b) The investigated impeller types

### CFD model of the stirred vessel

The Rotating Machinery model of COMSOL Multiphysics was used to calculate the flow field within the vessel, which is described the motion of rotating parts with the help of Navier-Stokes equations augmented with  $k-\epsilon$  turbulence model. A detailed description about the correlations built into the applied model is discussed in article of Kumaresan et al. [25]. The model can be used to study the dynamic behaviour of the vessel. The vessel was modelled in 3D, because the impellers did not allow reducing the number of space coordinates. Three, four, five and six-blades Rushton turbines (show in Figure 1(b)) were investigated based on experimental and simulation results. The geometry was split into a large number of finite elements to reach the required computational precision without a huge computational demand. Ethylene-glycol was used in experiments because the properties of this fluid notably depend on temperature (shown in Figure 2). In order to gather sufficient information about the calculated velocity field all the geometry axes were divided into 10 equidistant parts. The calculated velocity magnitudes were collected in the resulted intersection points (shown in Figure 3).

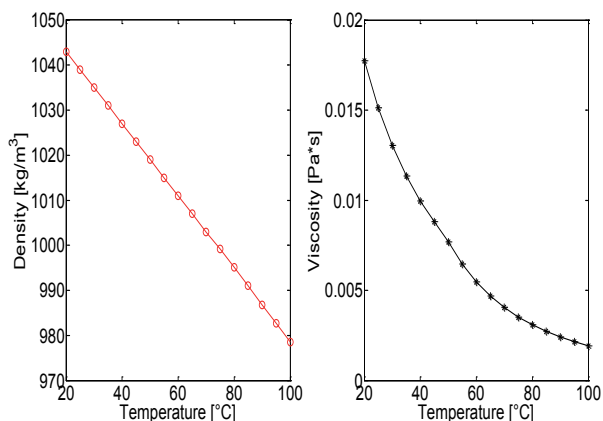


Fig. 2. Density and viscosity of ethylene-glycol

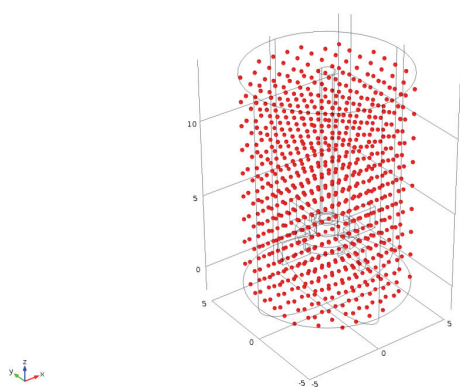


Fig. 3. Intersection points for velocity value extraction

The simulations and experiments were carried out at 50-500  $\text{min}^{-1}$  rotational speeds with the resolution of 50  $\text{min}^{-1}$ . The effect of the material properties on the electric power consumption was investigated in the temperature range of 20°C to 90°C with 10°C steps.

The extracted velocity averages from the simulation were plotted in histograms, with each impeller, at each rotational speed. The logarithmic abscissa in resulted histograms represents the velocity values, and the ordinate represents the frequency of these velocity values in the whole flow field.

Equation (7) was used to calculate the electric power requirement from the simulated results.

$$P = r \cdot \omega \cdot c_f \cdot \left( \iint \frac{\rho}{2} \cdot u^2 dx dy \right) \quad (7)$$

Tab. 1. Parameters for Equation (8) at three temperatures for three- and six-bladed Rushton turbines

Parameter\ Temperature (°C)	Three-bladed Rushton turbine			Six-bladed Rushton turbine		
	20	50	90	20	50	90
x	$1.99 \cdot 10^{-4}$	$3.94 \cdot 10^{-5}$	$4.77 \cdot 10^{-6}$	$1.59 \cdot 10^{-4}$	$4.15 \cdot 10^{-5}$	$4.39 \cdot 10^{-6}$
y	$-6.71 \cdot 10^{-2}$	$-3.01 \cdot 10^{-2}$	$-1.08 \cdot 10^{-2}$	$-6.08 \cdot 10^{-2}$	$-3.11 \cdot 10^{-2}$	$-1.01 \cdot 10^{-2}$
z	1.26	1.43	1.75	$7.12 \cdot 10^{-1}$	$8.14 \cdot 10^{-1}$	$8.53 \cdot 10^{-1}$

The surface integral in the parenthesis represents the force awakened on the surface of the blades. This force multiplied by the length of the lever arm, in this case the length of the mixing blades ( $r$ ), result in torque. The torque multiplied by the angular velocity ( $\omega$ ) results in power requirement of the impeller at a defined rotational speed. Dimensionless resistance factor,  $c_f$  in Equation (8) must be determined in an experimental way [26]. The resistance factor is related to the properties of the mixed material. We used the following equation to describe the resistance factor as the function of Reynolds number:

$$c_f = x \cdot \text{Re}^2 + y \cdot \text{Re} + z \quad (8)$$

The constants (shown in Table 1) in Equation (8) were determined with a parameter identification applying a global search algorithm (Particle Swarm Optimization) based on experimental data, the measured torque values [27]. In Equation (8)  $\text{Re}$  is the dimensionless Reynolds-number, that gives a measure of the ratio of inertial forces to viscous forces and consequently quantifies the relative importance of these two types of forces for given flow conditions.  $\text{Re}$  is determined based on the simulation results as the surface average of the calculated Reynolds-number on one blade at each rotational speed.

## Results

### Homogeneity calculation using histograms

To characterize the developed histograms of homogeneity, mean values and standard deviation was calculated for the easier comparability. The standard deviation is an absolute and not a relative value, so to get the normalized standard deviation, standard deviation value was divided with the mean value and multiplied by one hundred. For demonstration the results were shown in Figure 4 at 20°C (a), 50°C (b), and 90°C (c) with the rotational speeds 50  $\text{min}^{-1}$ , 250  $\text{min}^{-1}$  and 500  $\text{min}^{-1}$ . Figure 4 shows the histograms of the homogeneity of the unit resulted by a Rushton turbine with three blade at these temperatures and rotational speeds. As it is expected with the increasing of rotational speed the mean values (MV) are increased at every case. Comparing the normalized standard deviations (NSTD) shows that with the increase in the rotational speed from 50  $\text{min}^{-1}$  to 500  $\text{min}^{-1}$  the variance decreases from 116% to 22%. This tenfold rise of the rotational speed results a more than five times better homogeneity in the system. This improvement in the homogeneity falls off at higher temperatures, because the

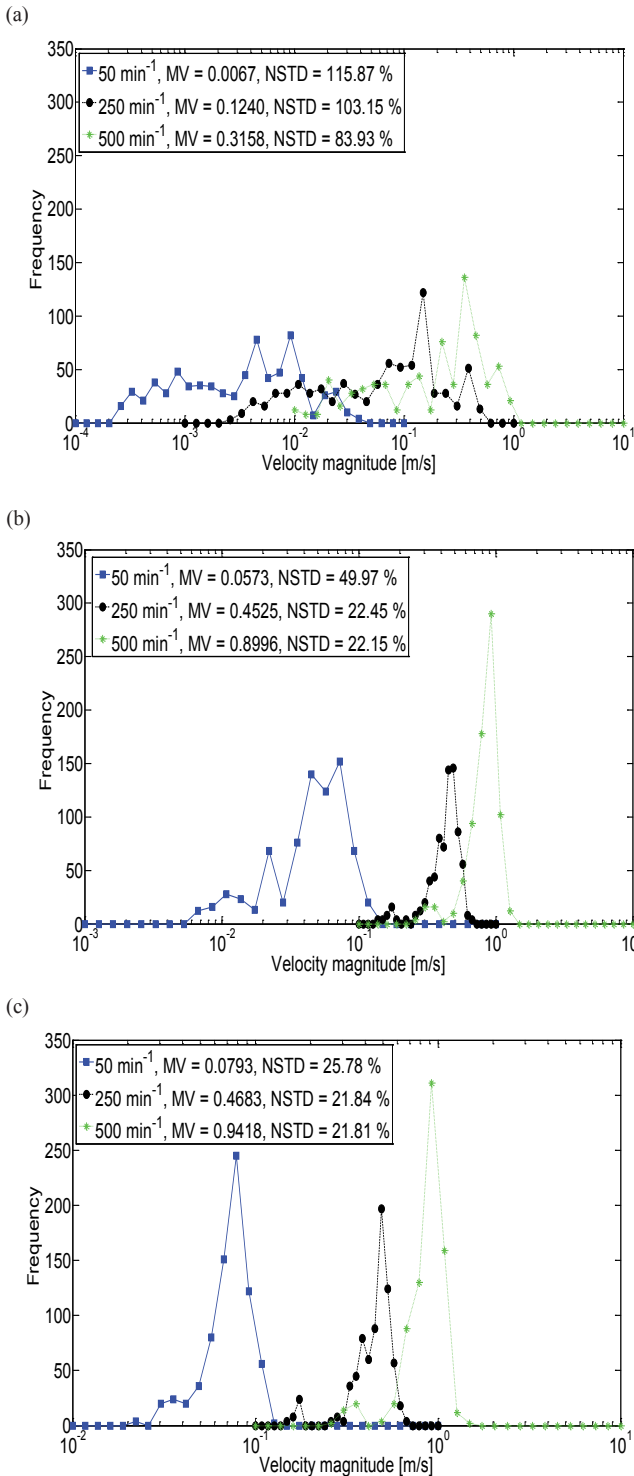


Fig. 4. (a) Effect of rotational speed on the homogeneity resulted by a three-bladed Rushton turbine at 20 °C, (b) at 50°C, (c) and at 90°C

higher viscosity renders more difficult mixing at lower temperatures. It can be seen too, that at the 500 min<sup>-1</sup> the viscosity has no effect on the variance, only the mean value changes.

In Figure 5 the effect of the rotational speed and the temperature is shown for a reactor with a six-bladed Rushton turbine. The results are similar to the ones that can be seen in Figure 4, but the changes are lower than the three-bladed turbine. At 20°C, if the rotational speed is gone up from 50 min<sup>-1</sup> to 500 min<sup>-1</sup>, the improvement in homogeneity is less than the case of the three

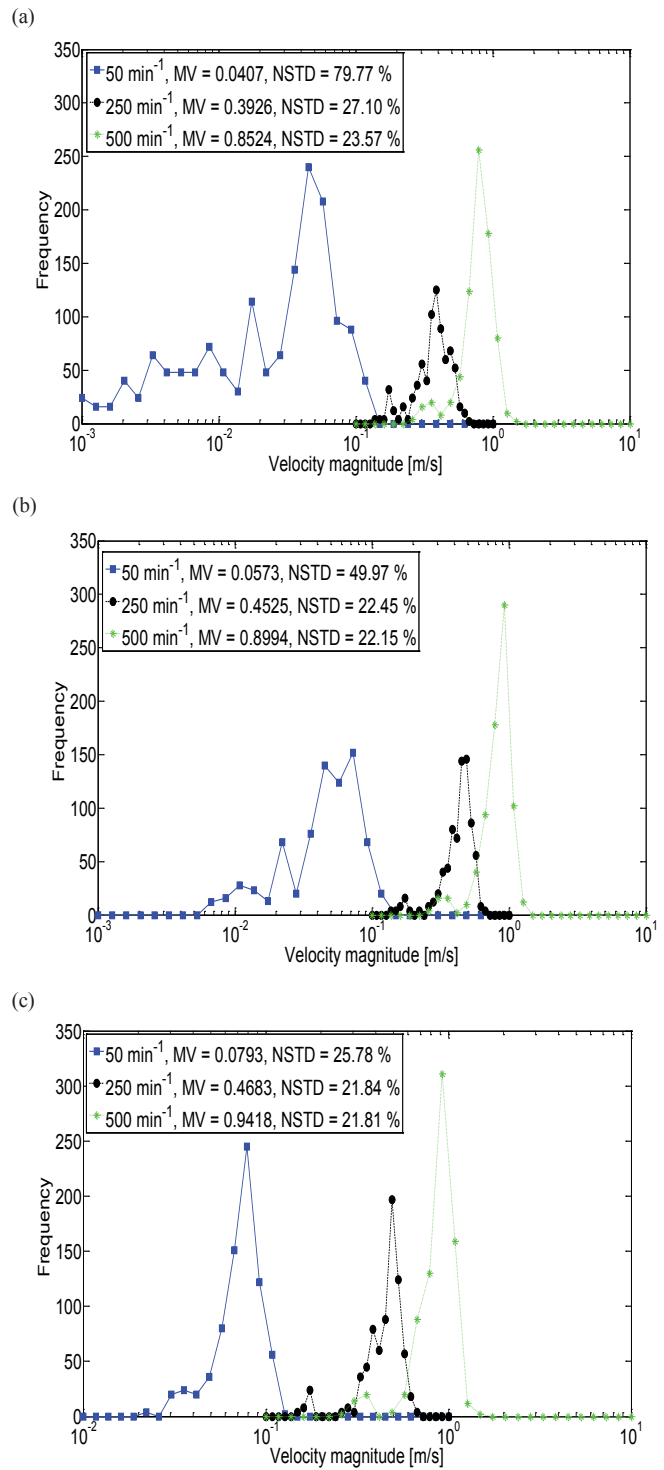
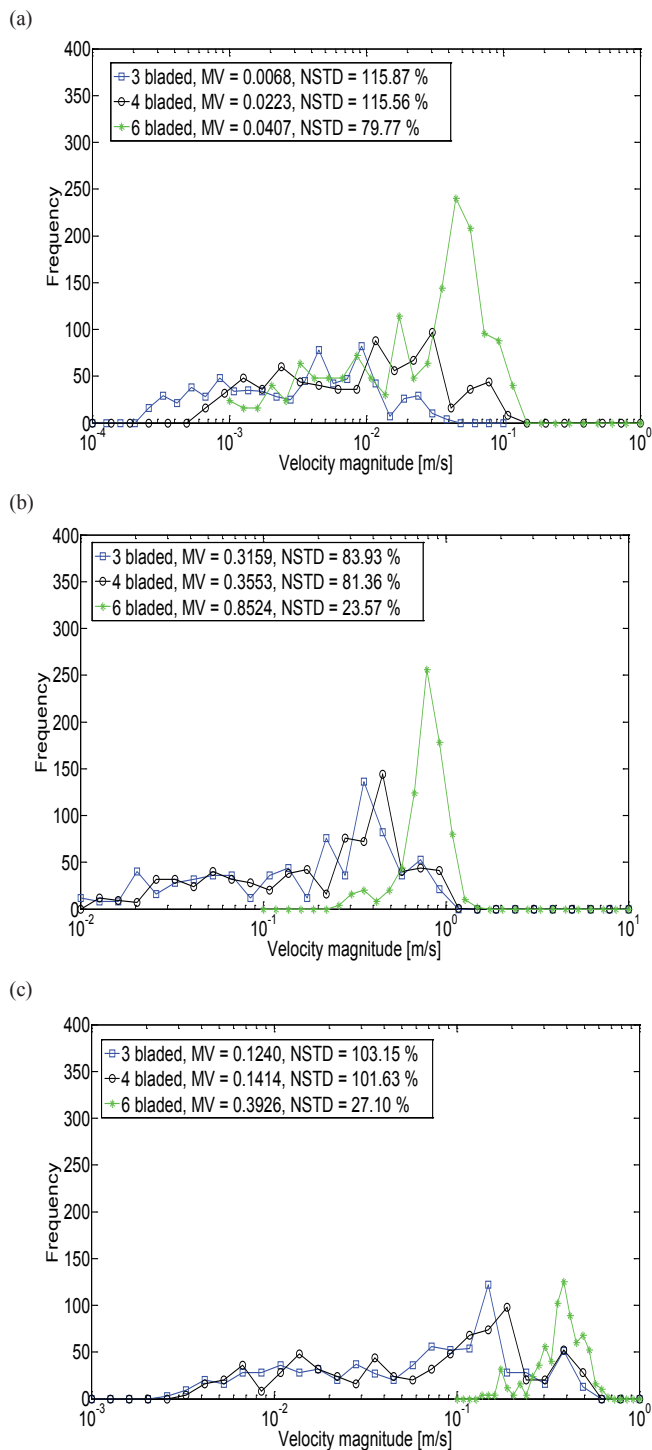


Fig. 5. (a) Effect of rotational speed on the homogeneity resulted by a six-bladed Rushton turbine at 20°C, (b) at 50°C, (c) and at 90°C

bladed Rushton turbine. In this case the variance is progressed from 80% to 24%. This happened because the six-bladed Rushton turbine is more effective on lower rotational speeds than the three-bladed one. The improvement falls off at 50°C (two times) and at 90°C (cc. equal). At a given rotational speed as the temperature is increased the NSTD shows the homogeneity is 80% at 20°C and 26% at 90°C. This correspondence at 500 min<sup>-1</sup> is 23% to 22%. So we can see that the homogeneity is independent from the viscosity at high rotational speeds.



**Fig. 6.** Effect of the changes in the blade number on the homogeneity at 20°C and at (a) 50 min<sup>-1</sup>, (b) 250 min<sup>-1</sup> and (c) 500 min<sup>-1</sup>

The effect of the blade number was examined too at 20°C. For demonstration the three, five, and six-bladed Rushton turbine were used. The results are shown in Figure 6. It can be seen that the three- (a) and five-bladed (b) Rushton turbines have always worse performance than the six-bladed (c) one. The variance is 116% for the three-bladed form, 113% for the five-bladed form and 80% for the six-bladed form at 50 min<sup>-1</sup>. A huge gap is experienced between Rushton turbines with five- and six-bladed at each rotational speed. The width of this gap is decreased by the increasing of the rotational speed, but at 250 min<sup>-1</sup> and 500 min<sup>-1</sup> the gap is stayed unchanged.

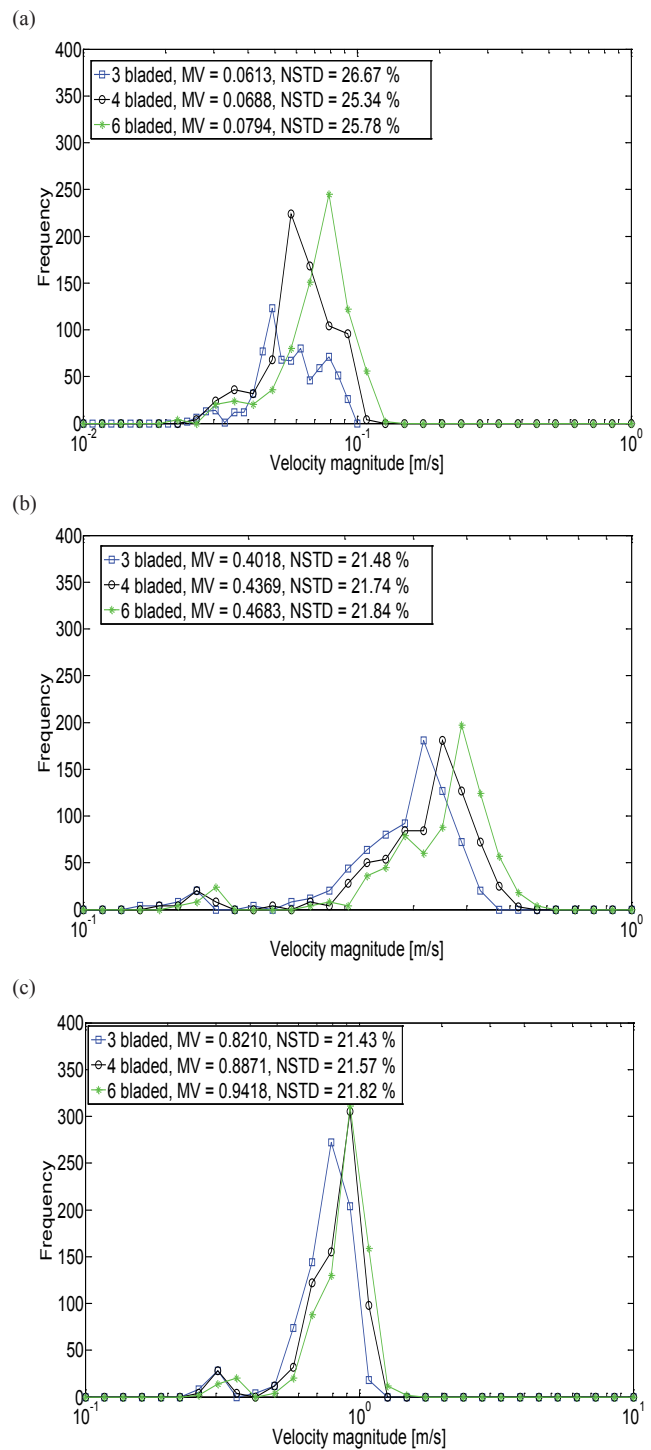


**Fig. 7.** Effect of the changes in the blade number on the reactor homogeneity at 90°C and at (a) 50 min<sup>-1</sup>, (b) 250 min<sup>-1</sup> and (c) 500 min<sup>-1</sup>

The effect of the changes in the blade number at 90°C can be seen in Figure 7. The difference from the Figure 6 is significant. At high temperatures, the viscosity is lower too and the homogeneity does not depend on the rotational speed, because it can be mixed well at lower rotational speeds. The blade number has only a little influence on the NSTD values. Hence, for mixing high viscosity fluids with Rushton turbine, it can be stated, that increasing the blade number of the impeller is not worthy, because it has no effect on the improvement if the homogeneity of the reactor.

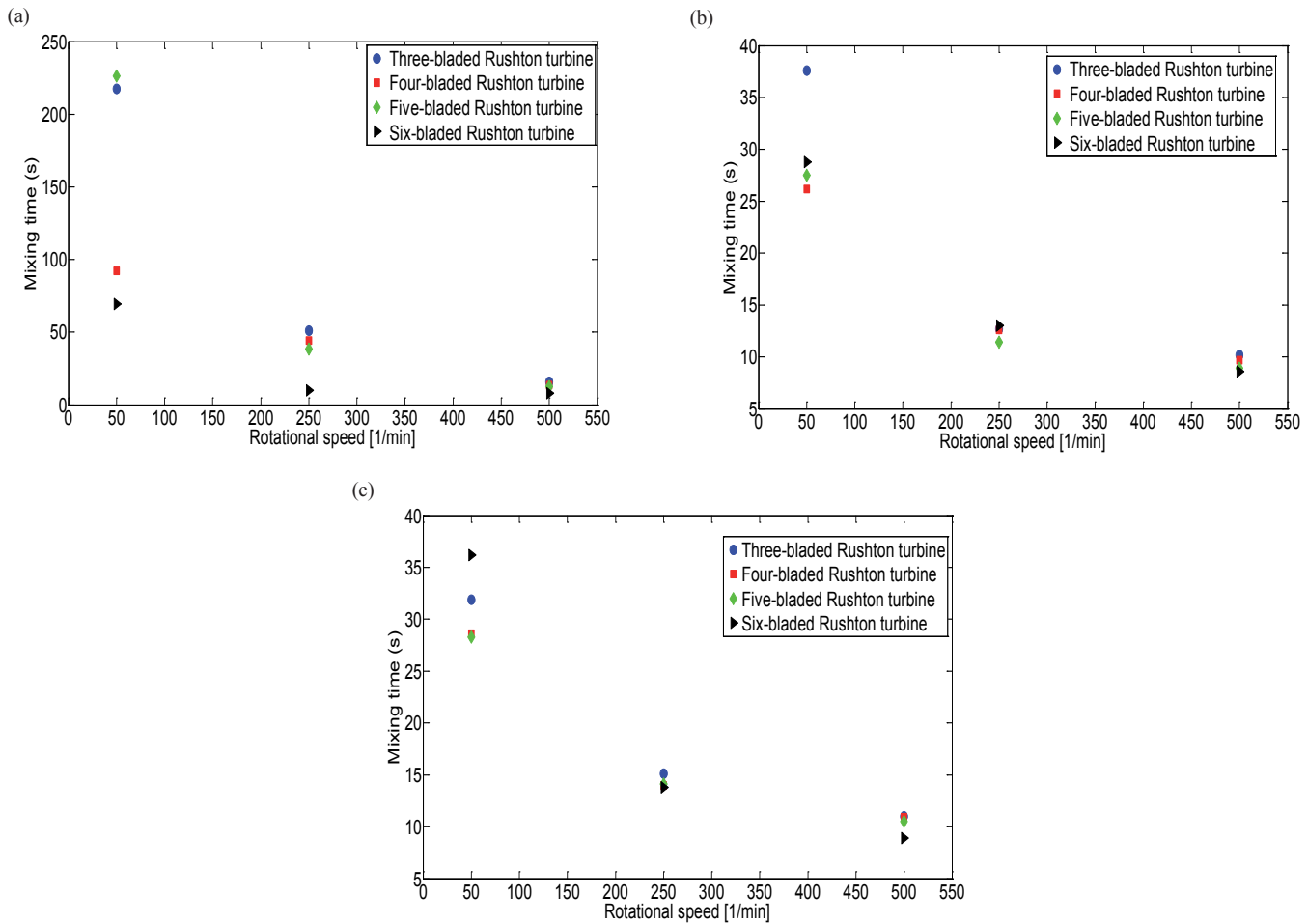


Fig. 8. Effect of the changes in the blade number on the mixing time at (a) 20°C, (b) 50°C and (c) 90°C

### Mixing time

The histogram based evaluation method of the velocity field in stirred tank is not widespread in the industry. In order to show that this method can be useful to quantify the effect of different mixing geometries, mixing time was analysed through simulation. The modelling method is described in detail in previous publications [28,29]. In Figure 8 the effect of the blade number and the temperature on the mixing time can be seen. From 50 min<sup>-1</sup> to 250 min<sup>-1</sup>, the improvement of the rotational speed has a huge effect on reducing the time needed to reach the homogeneity of 95%. That can be noticed, that at lower rotational speed and 20°C, the mixing time is higher at least two times than at higher temperatures. At high rotational speed, viscosity has no significant effect on the mixing time, and it can be seen that the increase of the blade number results better and better mixing times. As we can make the same conclusions than we stated earlier based on the developed histograms it can be mentioned that the suggested characterization method can be applied in the quantified characterization of the homogeneity.

### Power requirement

As we earlier mentioned a correlation was defined to describe the resistance factor in which there are three unknown parameters

identified and collected in Table 1. The identified parameters were used in Equation (8). In Figure 9-10 the comparison of experimental and calculated power consumption can be seen for three- and six-bladed Rushton turbines. Based on the fitting it can be stated that the developed CFD model can be applied to calculate the electric consumption of the mixer. As it was seen if the rotational speed is increased from 50 min<sup>-1</sup> to 500 min<sup>-1</sup> at 20°C in case of the three-bladed Rushton turbine the homogeneity will be more than five times better. For a six-bladed Rushton turbine to increase the homogeneity of the stirred vessel four times, it is need also ten times improvement in the electric power consumption. To achieve this improvement in the homogeneity cc. tenfold increase in electrical power consumption of the motor is required. It can be seen too, that from 200 min<sup>-1</sup> and 400 min<sup>-1</sup> the effect of the increase in the rotational speed does not result significant rise in the power consumption of the mixer, but if we want to operate the impeller at lower or higher rotational speeds a little change in the rotational speed can be issued in a large change in the power consumption.

Power number is a commonly-used dimensionless number relating the resistance force to the inertia force. On Figure 11 Power number versus the Reynolds number can be seen on a log-log diagram in the case of three- (a) and six-bladed (b) Rushton

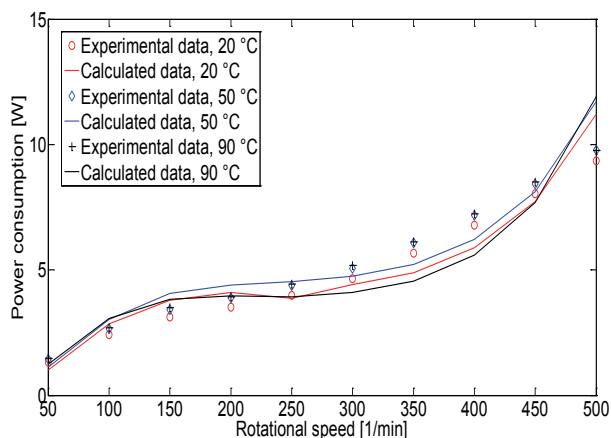


Fig. 9. Comparison of experimental and calculated electric power consumption with the three-bladed Rushton turbine

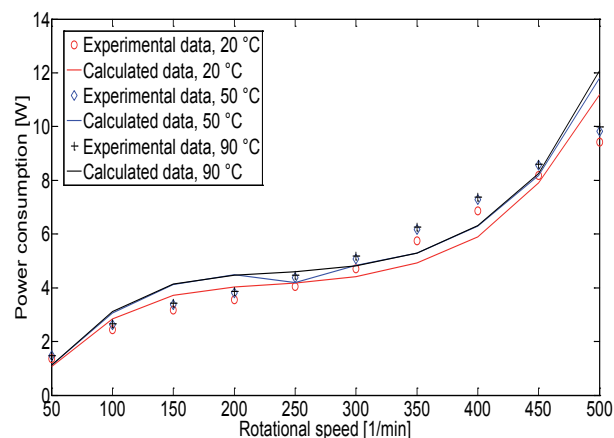


Fig. 10. Comparison of experimental and calculated electric power consumption with the six-bladed Rushton turbine

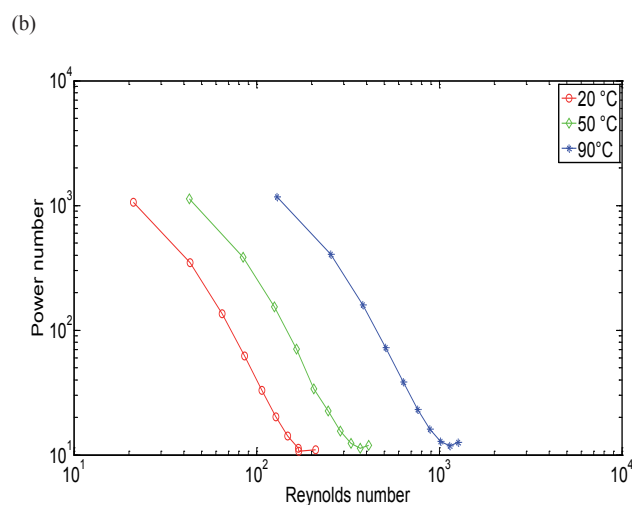
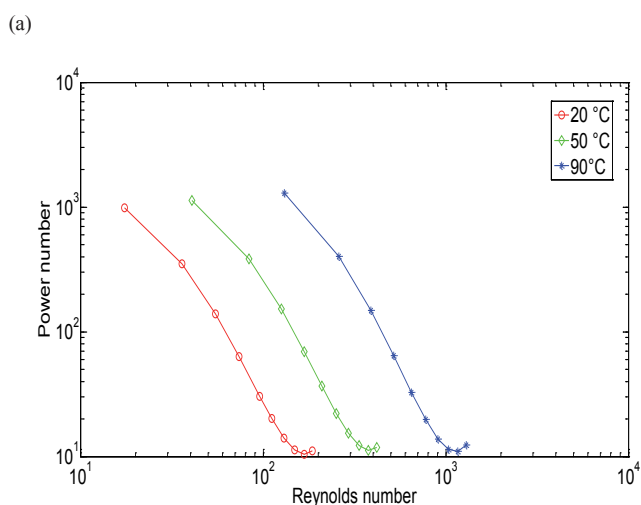


Fig. 11. Power number versus Reynolds number (a) in case of three-bladed Rushton turbine, (b) in case of six-bladed Rushton turbine

turbines, at different temperatures. The calculations based on the developed CFD models. It can be seen that the Power number is very strongly affected by the rotational speed, and material properties. Similar results can be seen in the literature [31] which also suggests that the developed models are valid.

### Conclusions

Homogeneity of the velocity field, mixing time, power number and power consumption were studied in a stirred equipment. Four different impeller geometries (three-, four-, five-, and six-bladed Rushton turbine) were investigated at many rotating speeds, and three temperatures. Homogeneity of the velocity field in the vessel was plotted on logarithmic histograms. As it was shown the homogeneity was depended on the temperature and the rotational speed. The blade number of the

Rushton turbine shows great difference in the achieved homogeneity of the mixed phase. Mixing time was calculated to see how much time is needed to reach a 95% homogeneity. The rotational speed has huge effects on lower the mixing time if rotational speeds lower than 250 min<sup>-1</sup>.

To study the power consumption of the mixer, a laboratory mixed system was built. The  $c_f$  dimensionless resistance factor was determined with parameter identification to calculate the power consumption. The simulated electric power consumption was compared to the experimental ones and a proper fitting was experienced. Power number was calculated too which shows similar results to the literature. Further research is needed to define optimal rotational speed for each impeller type, and to expand the number of the investigated impeller geometries.

## Notation

$D$	Impeller diameter [m]	$g$	Gravitational acceleration $\left[\frac{m}{s^2}\right]$
$T$	Tank diameter [m]	$g_c$	Newton's law conversion factor
$Z$	Liquid depth [m]	$v$	Velocity $\left[\frac{m}{s}\right]$
$C$	Clearance of impeller off vessel bottom [m]	$L$	Characteristic length [m]
$w$	Blade width [m]	$\Delta p$	Pressure difference [Pa]
$p$	Pitch of blades [m <sup>2</sup> ]	$a_{1,2,3}$	parameters
$n$	Number of blades	$r$	Blade length [m]
$\rho$	Density $\left[\frac{kg}{m^3}\right]$	$\omega$	Angular velocity $\left[\frac{rad}{s}\right]$
$\mu$	Kinematic viscosity [Pa · s]	$c_f$	Resistance factor
$P$	droplet surface [m <sup>2</sup> ]	$x$	Constant
$N$	Power [W]	$y$	Constant
		$z$	Constant

## Acknowledgements

This research was realized in the frames of TÁMOP 4.2.4. A/2-11-1-2012-0001 „National Excellence Program – Elaborating and operating an inland student and researcher personal support system.

## References

- 1 Tamburini A., Cipollina A., Micale G., Brucato A., Ciofalo M., *CFD prediction of solid particle distribution in baffled stirred vessels under partial to complete suspension conditions*. Chemical Engineering Transactions, 32, pp. 1447-1452, (2013). DOI: [10.3303/CET1332242](https://doi.org/10.3303/CET1332242)
- 2 Wei H., *Computer-aided design and scale-up of crystallization processes: integrating approaches and case studies*. Chemical Engineering Research and Design, 88 (10), pp. 1377-1380, (2010). DOI: [10.1016/j.cherd.2009.07.020](https://doi.org/10.1016/j.cherd.2009.07.020)
- 3 Rudniak L., Machniewski P. M., Milewska A., Molga E., *CFD modelling of stirred tank chemical reactors: homogeneous and heterogeneous reaction systems*. Chemical Engineering Science, 59 (22-23), pp. 5233-5239, (2004). DOI: [10.1016/j.ces.2004.09.014](https://doi.org/10.1016/j.ces.2004.09.014)
- 4 Sommerfeld M., Decker S., *State of the art trends in CFD simulation of stirred vessels*. in 'Proceedings of the 11th European Conference on Mixing, Bamberg', 1, (2003).
- 5 Hippler, J. E., *B.Ch.E. Thesis, Department of Chemical Engineering, Villanova University, Villanova, Pennsylvania, (1956)*.
- 6 Johnstone R. E., Thring M. W., *Pilot plants, models and scale-up methods in chemical engineering*. McGraw-Hill, New York (1957).
- 7 Rushton J. H., Costich E. W., Everett H. J., *Power characteristics of mixing impellers I*. Chemical Engineering Progress, 46 (8), pp. 395-404, (1950).
- 8 Bird R. B., Stewart W. E., Lightfoot E. N., *Transport phenomena*. Rev. 2. ed. Wiley, New York (2007).
- 9 Schlichting H., *Boundary layer theory*. McGraw-Hill, New York (1960).
- 10 Bader F. G., *Modelling mass transfer and agitator performance in multiturbine fermentors*. Biotechnology and Bioengineering, 30 (1), pp. 37-51 (1987). DOI: [10.1002/bit.260300107](https://doi.org/10.1002/bit.260300107)
- 11 Brown D. E., *The measurement of fermentor power input*. Chemistry & Industry, 16, pp. 684-688, (1997).
- 12 Oosterhuis N. M. G., Kossen N. W. F., *Power input measurements in a production scale bioreactor*. Biotechnology Letters, 3 (11), pp. 645-650, (1981). DOI: [10.1007/BF00158694](https://doi.org/10.1007/BF00158694)
- 13 Holland F. A., Chapman F. S., *Liquid mixing and processing in stirred tanks*. Reinhold, New York, (1966).
- 14 Machon V., Vlcek J., Shrivaneck J., *Dual impeller systems for aeration of liquids: an experimental study*. in 'Proceedings of 5th European conference on Mixing BHRA Fluid Engineering, Cranfield Institute, Bedford, UK', pp. 155-169, (1985).
- 15 Himmelstein S., *Precision torque meter readouts, bulletin 360D*. Himmelstein & Co., Hoffman Estates, (1998).
- 16 Chatwin S., Nienow A. W., *Successful power measurement in agitated vessels*. Laboratory Science and Technology, September, 19, (1985).
- 17 Wang W., Zhao S., Shao T., Jin Y., Cheng Y., *Visualization of micro-scale mixing in miscible liquids using  $\mu$ -LIF technique and drug nano-particle preparation in T-shaped micro-channels*. Chemical Engineering Journal, 192, pp. 252-261, (2012). DOI: [10.1016/j.cej.2012.03.073](https://doi.org/10.1016/j.cej.2012.03.073)
- 18 MacTaggart R. S., Nasr-El-Din H. A., Masliyah J. H., *A conductivity probe for measuring local solids concentration in a slurry mixing tank*. Separations Technology, 3(3), pp. 151-160, (1993). DOI: [10.1016/0956-9618\(93\)80015-J](https://doi.org/10.1016/0956-9618(93)80015-J)
- 19 Paul E. L., Atiemo-Obeng V. A., Kresta S. M., *Handbook of industrial mixing: science and practice*. Wiley & Sons, Hoboken, New Jersey (2004).
- 20 Nurtono T., Setyawan H., Altway A., Winardi S., *Macro-instability characteristic in agitated tank based on flow visualization experiment and large eddy simulation*. Chemical Engineering Research and Design, 87 (7), pp. 923-942, (2009). DOI: [10.1016/j.cherd.2009.01.011](https://doi.org/10.1016/j.cherd.2009.01.011)

- 21 **Van de Vusse J. G.**, *Mixing by agitation of miscible liquids Part I*. Chemical Engineering Science, 4 (4), pp. 178-200, (1955).  
DOI: [10.1016/0009-2509\(55\)85020-8](https://doi.org/10.1016/0009-2509(55)85020-8)
- 22 **Spero P. M.**, *Thermocouple temperature measurements for twin jet thermal mixing*. Master's dissertation, University of Tennessee (2011).
- 23 **Kramers H., Baars G. M., Knoll W. H.**, *A comparative study on the rate of mixing in stirred tanks*. Chemical Engineering Science, 2 (1), pp. 35-42, (1953).  
DOI: [10.1016/0009-2509\(53\)80006-0](https://doi.org/10.1016/0009-2509(53)80006-0)
- 24 **Hayes R. E., Afacan A., Boulanger B., Tanguy P. A.**, *Experimental study of reactive mixing in a laminar flow batch reactor*. Chemical Engineering Research and Design, 76 (1), pp. 73-81, (1998).  
DOI: [10.1205/026387698524497](https://doi.org/10.1205/026387698524497)
- 25 **Kumaresan T., Joshi J. B.**, *Effect of impeller design on the flow pattern and mixing in stirred tanks*. Chemical Engineering Journal, 115 (3), pp. 173-193, (2006).  
DOI: [10.1016/j.cej.2005.10.002](https://doi.org/10.1016/j.cej.2005.10.002)
- 26 **Lazauskas L. V.**, *Hydrodynamics of advanced high-speed sealift vessels*. Master Thesis, University of Adelaide (2005).
- 27 **Birge B.**, *PSOt – a particle swarm optimization toolbox for use with Matlab*. in ,Swarm Intelligence Symposium. Indianapolis, Indiana, USA', pp. 182-186, (2003).
- 28 **Egedy A., Varga T., Chován T.**, *Particle tracing based model validation for CFD models of stirred reactors*. Chemical Engineering Transactions, 32, pp. 1429-1434, (2013).  
DOI: [10.3303/CET1332239](https://doi.org/10.3303/CET1332239)
- 29 **Egedy A., Varga T., Chován T.**, *CFD modelling and video analysis based model validation for a stirred reactor*. Computer Aided Chemical Engineering, 30, pp. 1123-1127, (2012). ISBN 978-0444-59431-0
- 30 **Bonvillani P., Ferrari M. P., Ducrós E. M., Orejas J. A.**, *Theoretical and experimental study of the effects of scale-up on mixing time for a stirred-tank bioreactor*. Brazilian Journal of Chemical Engineering, 23 (1), pp. 1-7, (2006).  
DOI: [10.1590/S0104-66322006000100001](https://doi.org/10.1590/S0104-66322006000100001)